Trajectories of the single moving equivalent dipole in subjects with left fascicular block

Vito Starc[1], Cees A Swenne[2]

[1]University of Ljubljana, Faculty of Medicine, Ljubljana, Slovenia
[2]Cardiology Department, Leiden University Medical Center, Leiden, The Netherlands

Abstract

At CinC 2017 we presented an application based on a spherically bounded model with homogeneous volume conductor to determine location, orientation and strength of a single moving equivalent dipole (SMED) in 12-lead ECGs. To initially explore its potential clinical use, we wanted to verify that the SMEDs in conduction defects will *be in other locations than those in a healthy heart.*

Using ECG criteria of AHA/ACCF/HRS, we studied subjects with left anterior fascicular block (LAFB, n=10) and subjects with left posterior fascicular block (LPFB, n=17), and contrasted these with subjects with normal ECGs (n=42). The SMEDs were assessed in 5-min supine resting 12-lead ECGs with a time resolution of 1 ms.

The spatial orientation of the heart's electrical axis through the centers of the derived SMED locations of the P wave and the QRS was found to be similar to that obtained by MRI studies. It was shown that the direction of the SMED trajectory and the SMED orientation rotate in the opposite sense and with different patterns in LAFB and LPFB, suggesting that the method could participate to the extension of discrimination criteria in both blocks.

This initial study with SMED assessment shows promising so far unexplored ECG-derived information. Further research in ECGs with various pathology is needed to investigate its possible diagnostic applicability.

1. Introduction

At CinC 2017 we presented an application based on a spherically bounded model with homogeneous volume conductor to determine location, strength, and orientation of a single moving equivalent dipole (SMED) in 12-lead ECGs [1]. To initially explore its potential clinical use, we wanted to verify that the SMEDs in conduction defects will be in other locations than those in a healthy heart. To this purpose, we studied ECGs with left fascicular blocks using the above model.

2. Subjects and methods

Using the model we studied subjects in sinus rhythm that satisfied ECG criteria for the left anterior fascicular block (LAFB, n=15) and those for the left posterior fascicular block (LPFB, n=17), and contrasted these with apparently healthy individuals with normal ECGs, excluding athletes (n=89). According to AHA/ACCF/HRS recommendation [2], the criteria for LAFB included frontal plane axis between -45° and -90°, qR pattern in lead aVL, R-peak time in lead aVL of 45 ms or more, and QRS duration less than 120 ms, whereas those for LPFB considered frontal plane axis between 90° and 180° in adults, rS pattern in leads I and aVL, qR pattern in leads III and aVF, and QRS duration less than 120 ms. All subjects were selected from our database used previously [3], containing an unselected group of 1050 subjects.

2.1. Determination of the SMEDs

In our model representing the electrical activity of the heart derived from the general solution of Laplace's equation, surface potentials are proportional to the dot product of the dipole and the lead vectors of the 12-lead ECG. The model estimates (inverse solution) the dipole and its location by minimizing the objective function that represents the error between the calculated model potentials and the measured potentials, determined with respect to Wilson's central terminal. Potentials are obtained at the electrode locations of the standard 12-lead ECG on the spherical surface with a radius of 15 cm, adapted to a template torso.

The SMEDs were determined in 5-min supine resting 12-lead ECGs with a time resolution of 1 ms (Cardiax/Cardiosoft). To eliminate the superposition of the T wave on P wave in each signal, the T wave was subtracted from the P wave (T wave cancellation) in the interval before the QRS onset. For each ECG sample, 9 potentials (VR, VL, VF, V1..V6) were used to determine the corresponding SMED (dipole strength, orientation, and its location).

2.2. A model of the left ventricle for the study of the SMED dynamics

To study the position and orientation of SMEDs with respect to the ventricular walls, a heart model with its 3-D orientation was necessary to build. The left ventricle (LV) was represented as a rotational ellipsoid with the short axis (b=3.5cm) rotated around its long axis (a=5cm) and truncated at the valvular plane 1.5 cm above the ellipsoid origin. The right ventricle was represented similarly, using only one half of the longitudinally cut ellipsoid attached to the LV at the intraventricular sulci. We assumed that the long axis of our model heart is oriented similarly to that one based on data from Odille F et al [5]. Using their data, we estimated the elevation (-21.3°) and azimuth (-57.1°) of the long axis with respect to the transverse plane and used these values as referential for our model heart. The short axis was assumed to lie symmetrically regarding the model heart and in the axial plane.

We assumed that the SMED trajectory of the first 60 ms of QRS is centered at the origin of the ellipsoidal LV, and speculated that the center of SMEDs of atrial activation lies on the long axis of LV. By defining a line through both SMED centers, we estimated the orientation of the heart electrical axis [Fig. 1], expressed by its elevation and azimuth.

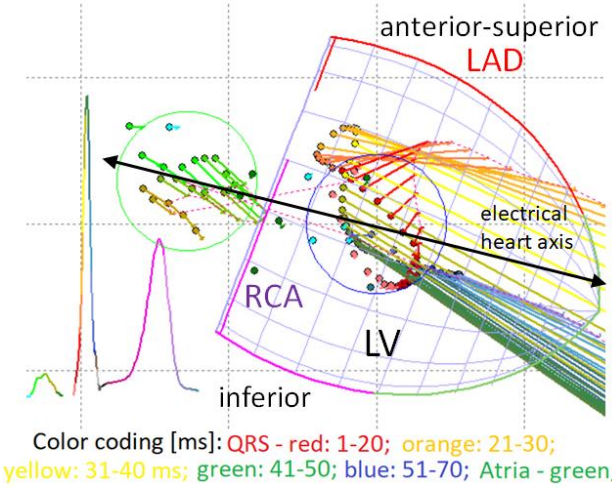

Figure 1. The electrical heart long axis (black line) and the referential model heart in the RAO view. The heart axis connecting the centers of the atrial and ventricular SMED locations (surrounded by green and red circles, respectively) is inclined by ~10° with respect to the referential model of the ventricles. Dipoles (strength) are presented by arrows (orientation) and closed circles (location), respectively. The SMED amplitude signal on the left has the same color coding as dipoles (the T wave is not shown). LAD, left anterior descending artery; RCA, right coronary artery;

2.3. SMED trajectory and SMED rotation

The SMED trajectories were constructed from a set of SMED locations providing the direction of movement, which was related to the instantaneous SMED orientation. It was evaluated by utilizing the planar angles ξ and ψ, of the direction of movement and the SMED orientation, respectively, obtained by projecting them onto a plane. Specifically, we used the atrioventricular (AV) plane (the LAO view), and the septal plane (the RAO view), with orientations given by the heart electrical axis. Both planar angles were gauged relative to the short axis.

The SMED trajectory exhibited a curvilinear path with the SMED orientation (planar angle ψ) in all directions with respect to the direction of movement (angle ξ). Several typical patterns emerged during the QRS. In the ψ flip pattern, a nearly linear trajectory path experienced a sudden change in planar angle ψ of up to 180° within 5 ms [Fig 2A]. The SMED trajectory often exhibited a trajectory loop (TL) with an angle ξ rotating either in the clockwise (ξ↓) [Fig. 2B] or in the counter-clockwise (ξ↑) sense [Fig. 2C]. It was accompanied by rotations in angle ψ (the SMED orientation) either in the clockwise (ψ↓) or in the counter-clockwise (ψ↑) sense.

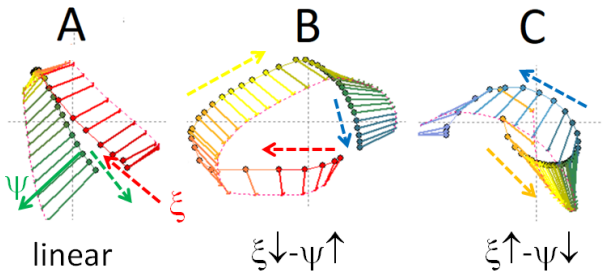

Figure 2. The dynamics of the SMED trajectory and the SMED orientation. The SMED orientation is shown by solid arrows (angle ψ), and the direction of the SMED movement (angle ξ) by broken colored arrows. A: The ψ flip pattern with a linear trajectory path in the AV plane. B, C: combined ξ↓-ψ↑ and ξ↑-ψ↓ patterns, respectively, both in the septal plane. See also Fig. 1.

To quantify changes ψ in our subjects, we determined the points P_1 and P_2 in the AV plane [Fig .3]. P_1 was defined at the time instant t_1 after the QRS onset when the SMED strength exceeded 10 % of the maximal value reached during QRS, and ψ attained the ψ_1. Though in many cases ξ exhibited a zig-zag pattern, ψ did not change considerably during the initial phase until the appearance of a ψ flip, which occurred at time t_2. Ten ms later (t_2+10 ms) at the point P_2, ψ was stabilized at the value of ψ_2. We also determined the distance d_{12} between the points P_1 and P_2 and the angle ξ_{12} from P_1 and P_2 in the AV plane.

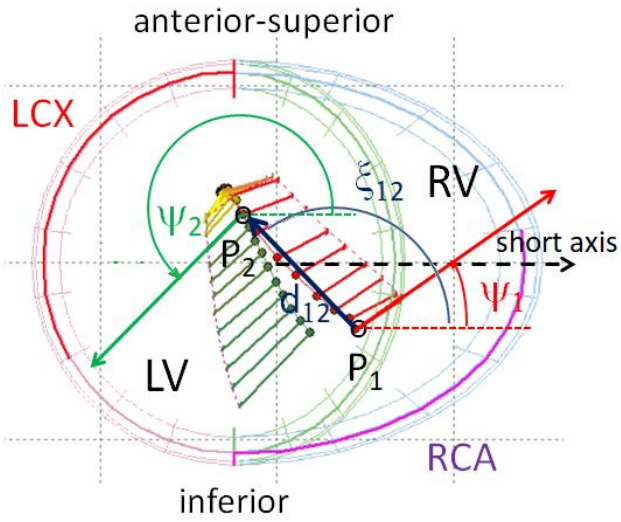

Figure 3. The model of LV in the AV plane (LAO view) with SMEDs of the first 70 ms of QRS. ψ_1 and ψ_2, orientation angles of the SMEDs located at P_1 and P_2; ξ_{12} and d_{12}, direction angle and distance from P_1 to P_2; LCX, the left circumflex artery. See also Fig. 1.

3. Results

The determination of the electrical heart long axis in space using the mean SMED locations of the P wave and QRS provided the value for elevation in the control group of -10.5° and those for azimuth of around -51.1° (Table 1), which are biased from the referential values of -21.3° and -57.1° by nearly 11° and 6°, respectively, but with similar variances. There were no statistically significant differences between the LAFB and LPFB groups vs. control except that for elevation between LAFB and Ctrl.

Table 1. SMED dynamics in the AV plane

Variable		^{0}*Ctrl*	^{1}*LAFB*	^{2}*LPFB*	p_{01}	p_{02}
N		89	15	18		
elevation	Mean	-10.5	-7.1	-11.6	0.007	0.50
	±SD	12.6	10.7	20.4	*	NS
azimuth	Mean	-51.1	-55.3	-51.2	0.84	0.99
	±SD	16.4	24.5	12.1	NS	NS

p_{01} and p_{02}: p values of the statistical significance for differences between the control and LAFB groups, and between the control and LPFB group, respectively

The results of the SMED dynamics in the AV plane are presented in Table 1. In the control group (Ctrl), P_1 was reached at time t_1 around 12.5 ms after the QRS onset with SMEDs directed mainly toward the septum and slightly anteriorly at the mean angle ψ_1 of 24°. The ψ flip occurred at flip around 28 ms with the angle ψ_2 of 203° reached at $t_2 = t_{flip}+10$ms when the trajectory covered the distance d_{12} of 1.89 cm in the direction ξ_{12} of 141° from P_1 to P_2. The SMED movement often exhibited a trajectory loop, mostly rotating in $\xi\uparrow$ and $\psi\uparrow$.

In the septal plane, TL rotation of the SMEDs existed in 46 (52%) cases all exhibiting $\xi\uparrow$, whereas in 33 (37%) cases the loop was either degenerated into two antiparallel lines or a ψ flip occurred. The rotation of the SMED orientation showed $\psi\uparrow$ pattern in 68 (76%) cases, and the ψ flip occurred in 11 (12%) cases. In the rest of the cases, the rotation was indeterminate. The most frequent combination of the rotation sense of the TL and ED orientation was $\xi\uparrow$-$\psi\downarrow$, appearing in 41 (46%) cases.

Table 2. Dynamics of the direction of the SMED trajectory and the SMED orientation in the AV plane

Pattern	^{0}*Ctrl*	^{1}*LAFB*	^{2}*LPFB*
N	89	15	18
$\xi\uparrow$	52%	0	94%
$\xi\downarrow$		87%	0
$\psi\uparrow$		73%	0
$\psi\downarrow$	76%	0	94%
$\xi\uparrow$-$\psi\downarrow$	46%	0	89%
$\xi\downarrow$-$\psi\uparrow$	0	73%	0

ξ, trajectory direction angle; ψ, SMED orientation angle; $\uparrow$, counter-clockwise; $\downarrow$, clockwise

In the LAFB group (N=15) the projection of the SMEDs orientation onto the AV plane showed that SMEDs of the initial phase was oriented statistically significantly more toward the inferior LV wall than in Ctrl (ψ_1: -50° vs. 24°, $p = 2.10^{-7}$), and those of the early middle phase more toward the anterosuperior wall than in Ctrl (ψ_1: 143° vs. 203°, $p = 2.10^{-7}$). In addition, SMEDs moved from P_1 to P_2 with a bigger ξ than in Ctrl (ξ_{12}: 210° vs 141°, p=0.004). In the septal plane (the RAO view), the dynamics of the SMED trajectories showed the following predominant patterns: $\xi\downarrow$ for TL rotation (13 cases, 87%), $\psi\uparrow$ for SMED orientation (11 cases, 73%), and $\xi\downarrow$-$\psi\uparrow$ (Fig. 2B) for a combination (13 cases, 87%).

In the LPFB group (N=18), the SMEDs P_1 projected onto the AV plane were oriented more toward the anterior-superior LV wall than in Ctrl (ψ_1 = +59° vs. 24°, $p = 3.10^{-6}$), and those at P_2 pointed toward the inferior wall (ψ_2 = 255 vs. 203°, $p = 10^{-5}$). The SMEDs moved from P_1 to P_2 in the direction of ψ_{12} = 208° (141° in Ctrl, p = 0.0015), covering a distance d_{12} =1.89 cm from P_1 (1.1 cm in Ctrl, p=0.0001). In the septal plane, the predominant patterns were: $\xi\uparrow$ for TL rotation (17 cases, 94%), $\psi\downarrow$ for the SMED orientation (17 cases, 94%), and $\xi\uparrow$-$\psi\downarrow$ (Fig. 2C) for a combination (16 cases, 89%).

4. Discussion and conclusion

This study demonstrates that application of a bounded spherical model for the description of the electrical activity of the heart using a SMED provides a distribution of dipoles, which is consistent with anatomical knowledge regarding the orientation of the heart's electrical long axis, and with the propagation of electrical excitation in the two types of left fascicular blocks compared to the normal spread of excitation. It introduces the concept of the SMED trajectory often forming a loop, of which rotation sense, in a combination with that of the SMED orientation, may help in discriminating the patterns of excitation in the heart.

Specifically, we found that the electrical heart axis obtained by our method is closely related to the spatial orientation of the anatomical axis of LV obtained by MRI [4], as suggested by a small bias between two methods of around 10° for the elevation angle and around 6° for the azimuth, and by comparable variances obtained from our study, and those of the angles θ^1_{AX} and θ^1_{CORO} [4] used in the derivation of the referential values. The deviation from the referential angles might have arisen due to anatomical misalignment of the center of the SMED trajectory in atria from the LV long axis as in Figure 1 or is due to different populations studied. This speculation could be tested using MRI. Though the method is very sensitive to deviations of ECG signal from the baseline, particularly in a low voltage P wave, it provided acceptable P wave SMED locations to get reasonable values for the orientation of the heart's electrical axis.

The orientation of a SMED with respect to a selected segment of the LV wall is more important than simply its orientation in 3-D space because it offers a ground for better physiological interpretation. Yet it requires that the derived SMED locations need to be at the right places within the heart, which might be affected by many approximations used in our model for determination of SMEDs, such as is a thorax in the form a spherical homogeneous conductor or inaccurate positions of the measuring electrodes. We only speculated that a mild distortion of space by those approximations would minimally affect mutual relative positions of SMEDs. Hence, by shifting of the center of the SMED trajectory to the center of the model LV, the SMEDs would be moved closer to their appropriate locations in the LV.

Our study showed that in LAFB SMEDs are oriented initially toward the inferior LV wall and after 30 to 40 ms nearly in the opposite direction, and that the SMED orientation during QRS rotates in the counter-clockwise sense, whereas in LPFB the behavior of SMEDs represent the exact mirror picture of LAFB, initially pointing to the anterior-superior LV wall and later nearly to the opposite direction, with a clockwise rotation of the SMED orientation. These findings that are all concordant with the vectorcardiographic view [5] support the validity of our method. In addition, with the finding that the SMED trajectory direction and the SMED orientation rotate in the opposite sense and with different patterns in LAFB and LPFB, our method could participate in extending of discrimination criteria in both blocks from the controls.

Despite apparently good results when separating individuals of the LAFB or LPFB group from the controls, a word of caution is necessary. Both groups with fascicular blocks are rather small, comprising around 1.5% of the initial population and with individuals selected retrospectively. Using stronger criteria for frontal axis deviation (>110°) than those of AHA/ACCF/HRS [2], Elizari et al [5] reported that pure LPFB is extremely rare, and mostly associated with the right bundle branch block. Retrospectively we found that 11 of 18 subjects were actively engaged in the sports, and only 3 of them satisfied the stronger ECG criteria for LPFB. When considering the finding that 46% of the controls exhibited the same $\xi\uparrow$-$\psi\downarrow$ pattern, prevalent in the LPFB group, it seems that majority of our LPFB subjects were not genuine, but rather satisfied (mild) criteria for LPFB. For more reliable results, a study with a larger LPFB group and stronger inclusion criteria should be performed.

By relating the SMED locations to the anatomy of the heart, our study provides suggestive evidence that our method for the assessment of the SMED location and orientation provides so far unexplored ECG-derived information. Further research in ECGs with various pathology is needed to investigate the possible applicability of this analysis in future ECG diagnostic algorithms.

References

[1] Starc V, Swenne CA. Spatial Distribution and Orientation of a Single Moving Dipole Computed in 12-Lead ECGs in a Healthy Population Using a Spherically Bounded Model. Computing Cardiol 2017; 44: pp.4.

[2] Surawicz B, Childers R, Deal BJ, Gettes LS, et al. AHA/ACCF/HRS recommendations for the standardization and interpretation of the electrocardiogram: part III. Circulation. 2009 Mar 17;119(10):e235-40..

[3] Starc V, Schlegel TT. Change in angular velocity at the end of the QRS loop aids the electrocardiographic detection of acute inferior myocardial infarction. Computing Cardiol 2015; 42: 601-4.

[4] Odille F, Liu S, van Dam P, Felblinger J. Statistical Variations of Heart Orientation in Healthy Adults. Computing Cardiol 2017; 44: pp. 4.

[5] Elizari MV, Acunzo RS, Ferreiro M. Hemiblocks revisited. Circulation. 2007 Mar 6;115(9):1154-63.

Address for correspondence.

Vito Starc, MD, PhD
Ljubljana University, Faculty of Medicine
Zaloska 4
SI 1104 Ljubljana, Slovenia
E-mail: vito.starc@mf.uni-lj.si